Geometric models for calculating cell biovolume and surface area for phytoplankton

JUN SUN* AND DONGYAN LIU

MARINE LIFE SCIENCE COLLEGE, OCEAN UNIVERSITY OF CHINA, QINGDAO 266003, CHINA

*CORRESPONDING AUTHOR: sunjun@ouc.edu.cn

Phytoplankton biovolume can be measured or calculated through the calculation of similar geometric models. A set of geometric models is suggested for calculating cell biovolume and surface area for 284 phytoplankton genera in China Sea waters. Thirty-one geometric shapes have been assigned to estimate the biovolume and surface area of phytoplankton cells. Reductions of error and microscopic effort are also discussed. The model has been verified by its application in the China Seas regions. The software to make these calculations is available at http://www.ouc.edu.cn/csmxy/sunjun/biovolume.htm

INTRODUCTION

The biovolume of marine phytoplankton cells is important to the study of phytoplankton ecology. The related parameters, such as cell size and conversion of carbon content from biovolume, and physiology functions are also important for marine ecosystem studies (Malone, 1980; Sournia, 1981; Chisholm, 1992).

Phytoplankton cell size varies greatly among different genera or even between different individuals. Sizes range from a few micrometres (or even less than 1 μm) to a few millimetres. Hence, there is a wide range of nine orders in magnitude for cell biovolume of phytoplankton. Several automated and semi-automatic methods for biovolume estimation have been described in the literature, such as the Coulter Counter (Hasting *et al.*, 1962; Maloney *et al.*, 1962; Boyd and Johnson, 1995), the micrographic image analysis system (Gordon, 1974; Krambeck *et al.*, 1981; Estep *et al.*, 1986; Verity and Sieracki, 1993; Sieracki *et al.*, 1998), flow cytometry (Olson *et al.*, 1985; Wood *et al.*, 1985; Steen, 1990; Cunningham and Buonnacorsi, 1992) and holographic scanning technology (Brown *et al.*, 1989). However, the general method for calculating phytoplankton cell biovolume is based on geometric assignation (Kovala and Larrance, 1966; Willén, 1976; Sicko-Goad *et al.*, 1977; Smayda, 1978; Edler, 1979; Rott, 1981; Kononen *et al.*, 1984; Vilicic, 1985; Hillebrand *et al.*, 1999). The methods mentioned above have advantages and/or disadvantages. Microscopic observation is a direct, convenient way to obtain species level information on phytoplankton taxa, whereas biovolume calculation based on geometric models of phytoplankton cells and their related conversion biomass are popular in phytoplankton ecology studies (Kuuppo, 1994; Snoeijs, 1994; Sommer, 1994, 1995; Tang, 1995; Hillebrand, 1997; Young and Ziveri, 2000). Some references (Smayda, 1978; Baltic Marine Environmental Protection Commission–Helsinki Commission, 1988; Hansen, 1992; Kramer *et al.*, 1992) list the biovolume calculations and their conversion biomasses as a routine method when studying phytoplankton.

Phytoplankton cell geometric models for biovolume calculation have been discussed in the literature (Kovala and Larrance, 1966; Willén, 1976; Edler, 1979; Rott, 1981; Kononen *et al.*, 1984; Hansen, 1992; Hillebrand *et al.*, 1999; Sun *et al.*, 2000a; Young and Ziveri, 2000). The method applies the principle of geometric models or shapes that are most similar to the real shape of the organism. Often there is the dilemma of whether to assign a phytoplankton cell shape to a complex but similar geometric model or to a simple, conveniently measurable, but inadequate model or shape. Most of the above studies pay attention to special regions or microalgae classes. Although different geometric equations used in the literature were dependent on dominance of the respective species in the local plankton communities, routine phytoplankton analysis would benefit from a series of standardized geometric models.

Hillebrand *et al.* recommend a standard set of 20 geometric shapes for over 850 genera and provide equations to be used for accurate estimates of cell volume and surface area for phytoplankton and microbenthic algae from linear dimensions measured microscopically (Hillebrand *et al.*, 1999). Its extensive listing of cell shapes will be a valuable resource for experimental and literature-based studies of relationships between cell size, surface area and biovolume for a wide variety of physiological characteristics. This comprehensive study will help set consistent parameters for evaluating the dynamics of phytoplankton standing stocks in terms of biovolume for ecological studies, and will be evaluated as a primary research reference in this field for studies of phytoplankton by physiologists and ecologists (Wheeler, 1999). Although it is comprehensive and extensive, its applicability is in need of expansion.

In the present study, based on earlier work of Hillebrand *et al.* (Hillebrand *et al.*, 1999), and focusing on phytoplankton species in the China Sea, a set of 31 geometric shapes is proposed for routine analysis of marine phytoplankton in China Sea waters. After consultation with the literature on phytoplankton studies in China's seas, we found that nearly 2000 taxa were recorded, belonging to 10 diverse groups and 284 genera (due to the volume of references, they cannot all be cited in this paper). Although the old nomenclature system is still in use in China, the checklist was modified according to Tomas (Tomas, 1997) (Table I). In order to improve the applicability of Hillebrand's geometric models, we reduced the number of microscopically measured line parameters, improving the previous shapes and updating the models. Furthermore, considering the fact that identifications of phytoplankton taxa need expert knowledge,

Table I: Shape codes of phytoplankton genera found in China Sea waters according to the geometric models in Table II

Genera	Shape code	Genera	Shape code
1. Cyanobacteria		*Xenococcus* Thuret	2
Anabaena Bory de St.-Vincent	1		
Aphanothece Näegeli	2	**2. Chrysophyceae**	
Arthrospira Stizenbberger	28	*Chromulina* Cienkowski	1
Borzia Cohn	28	*Dictyocha* Ehrenberg	1
Calothrix Agardh	28	*Dinobryon* Ehrenberg	2
Camptylonemopsis Desikachary	28	*Mallonmonas* Perty	2
Chlorogloea Wille	2	*Ochromonas* Wyssotski	9
Chroococcus Näegeli	1	*Synura* Ehrenberg	2
Chroothece Hansgirg	28		
Dichothrix Zanardini	28	**3. Bacillariophyceae**	
Enthophysalis Kützing	2	*Acanthoceras* Honigmann	29
Gardnerula de Toni	28	*Achnanthes* Bory de St.-Vincent	12
Gomphosphaeria Kützing	1	*Achnanthidium* Kützing	11
Homoeothrix (Thuret) Kirchner	28	*Actinocyclus* Ehrenberg	4
Hormathonema Ercegovic	2	*Actinoptychus* Ehrenberg	4
Hydrocoleum Kützing	28	*Amphipleura* Kützing	11
Hyella Bornet & Flahault	28	*Amphiprora* Ehrenberg	11
Isactis Thuret	28	*Amphora* Ehrenberg ex Kützing	17
Johannesbaptista de Toni	2	*Aneumastus* Mann & Stickle	11
Kyrtuthrix Ercegovic	28	*Anomoeoneis* Pfitzer	11
Lyngbya Agardh	28	*Anorthoneis* Grunow	11
Merismopedia Meyen	10	*Arachnoidiscus* Deane ex Pritchard	4
Microchaete Thuret	28	*Arcocellulus* Hasle, von Stosch & Syertsen	29
Microcoleus Desmazières	28	*Ardissonea* De Notaris	10
Microcystis Kützing	1	*Asterionella* Hassall	10
Nodularia Mertens	28	*Asterionellopsis* Round	10

(continued)

Table I: (continued)

Genera	Shape code	Genera	Shape code
Oscillatoria Vaucher	28	*Asterolampra* Ehrenberg	4
Phormidium Kützing	28	*Asteromphalus* Ehrenberg	4
Pleurocapsa Thuret ex Hauck	28	*Aulacodiscus* Ehrenberg	4
Richelia Schmidt	28	*Auliscus* Ehrenberg	11
Rivularia (Roth) Agardh	28	*Auricula* Castracane	17
Schizothrix Kützing	28	*Azpeitia* Peragallo	4
Scytonema Agardh	28	*Bacillaria* Gmelin	10
Sirocoleum Kützing	28	*Bacteriastrum* Shadbolt	28
Spirulina Turpin	28	*Bellerochea* Van Heurck emend. von Stosch	30
Symploca Kützing	28	*Biddulphia* Gray	29
Synechococcus Näegeli	1	*Bleakeleya* Round	10
Synechocystis Sauvageau	1	*Caloneis* Cleve	11
Tolypothrix Kützing	28	*Campylodiscus* Ehrenberg ex Kützing	11
Trichodesmium Ehrenberg	28	*Campyloneis* Grunow	11
Campylosira Grunow ex Van Heurck	14	*Grammatophora* Ehrenberg	10
Cerataulina Peragallo	28	*Guinardia* Peragallo	28
Cerataulus Ehrenberg	28	*Gyrosigma* Hassall	13
Chaetoceros Ehrenberg	29	*Hantzschia* Grunow	10
Chrysanthemodiscus Mann	5	*Helicotheca* Ricard	29
Cistula Cleve	11	*Hemiaulus* Ehrenberg	29
Climacodium Grunow	23	*Hemidiscus* Wallich	17
Climacosphenia Ehrenberg	31	*Hyalodiscus* Ehrenberg	1
Cocconeis Ehrenberg	11	*Hydrosera* Wallich	18
Corethron Castracane	5	*Isthmia* Agardh	29
Coscinodiscus Ehrenberg emend. Hasle & Sims	4	*Lauderia* Cleve	28
Cyclotella Kützing ex de Brébisson	4	*Leptocylindrus* Cleve	28
Cymatodiscus Hendey	4	*Leudugeria* Tempère ex Van Heurck	17
Cymatoneis Cleve	13	*Licmophora* Agardh	16
Cymatosira Grunow	29	*Lioloma* Hasle	10
Cymatotheca Hendey	17	*Liradiscus* Greville	4
Cymbella Agardh	17	*Lithodesmium* Ehrenberg	30
Dactyliosolen Castracane	28	*Luticola* Mann	11
Delphineis Andrews	11	*Lyrella* Karajeva	11
Denticula Kützing	11	*Martyana* Round	11
Detonula Schütt	28	*Mastogloia* Thwaites ex Smith	11
Diatoma Bory de St.-Vincent	29	*Mastogonia* Ehrenberg	11
Dictyoneis Cleve	12	*Melosira* Agardh	28
Dimeregramma Ralfs	29	*Meuniera* Silva	29
Diploneis Ehrenberg ex Cleve	12	*Minidiscus* Hasle	4
Ditylum Bailey ex Bailey	30	*Minutocellus* Hasle, von Stosch, & Syvertsen	11
Endictya Ehrenberg	4	*Navicula* Bory de St.-Vincent	11
Entomoneis Ehrenberg	12	*Neidium* Pfitzer	11
Ethmodiscus Castracane	4	*Nitzschia* Hassall	13
Eucampia Ehrenberg	29	*Nitzschiella* Rabenhorst	13
Eunotia Ehrenberg	15	*Odontella* Agardh	29
Eunotogramma Weisse	14	*Opephora* Petit	29
Eupodiscus Bailey	4	*Östrupia* Heiden ex Schmidt	11

(continued)

Table I: (continued)

Genera	Shape code	Genera	Shape code
Fallacia Stickle & Mann	11	*Palmeria* Greville	17
Fragilaria Lyngbye	29	*Paralia* Heiberg	4
Fragilariopsis Hustedt emend. Hasle	29	*Perissonoë* Andrews & Stoelzel	10
Frustulia Rabenhorst	11	*Petrodictyon* Mann	29
Gephyria Arnott	11	*Phaeodactylum* Bohlin	14
Gomphonema Agardh	21	*Pinnularia* Ehrenberg	10
Gomphonitzschia Grunow	21	*Plagiodiscus* Grunow & Eulenstein	14
Gossleriella Schütt	4	*Plagiogramma* Greville	11
Plagiogrammopsis Hasle, von Stosch & Syvertsen	29	*Tabularia* (Kützing) Williams & Round	10
Plagiotropis Pfitzer	11	*Tetracyclus* Ralfs	20
Planktoniella Schütt	4	*Thalassionema* Grunow	10
Pleurosigma Smith	13	*Thalassiosira* Cleve emend. Hasle	4
Pleurosira Trevison	28	*Thalassiothrix* Cleve & Grunow	10
Podocystis Bailey	11	*Toxarium* Bailey	24
Podosira Ehrenberg	5	*Trachyneis* Cleve	11
Proboscia Sundström	28	*Triceratium* Ehrenberg	18
Psammodictyon Mann	12	*Trigonium* Cleve	18
Psammodiscus Round & Mann	4	*Trinacria* Heiberg	18
Pseudoeunotia Grunow	4	*Tropidoneis* Cleve	11
Pseudo-nitzschia Peragallo	13	*Tryblioptychus* Hendey	11
Pseudosolenia Sundström	28	*Xanthiopyxis* (Ehrenberg) Ehrenberg	11
Pseudostaurosira (Grunow) Williams & Round	20		
Pyxidicula Ehrenberg	11	**4. Raphidophyceae**	
Rhabdonema Kützing	10	*Heterosigma* Hada	9
Rhaphoneis Ehrenberg	13	*Chattonella* Biecheler	9
Rhizosolenia Brightwell	28		
Rhoicosphenia Grunow	21	**5. Prymnesiophyceae**	
Rhopalodia Müller	17	*Acanthoica* Lohmann emend. Schiller and Kleijne	2
Rocella Hanna	4	*Calyptrolithia* Heimdal	2
Roperia Grunow ex Pelletan	11	*Emiliana* Hay & Mohler	1
Rossia Voigt	11	*Gephyrocapsa* Kamptner	1
Schroederella Pavillard	28	*Hayaster* Bukry	2
Scoliopleura Grunow	11	*Prymnesium* Massart ex Conrad	9
Sellaphora Mereschkowsky	10	*Syracosphaera* Lohmann	1
Skeletonema Greville	5		
Stauroneis Ehrenberg	29	**6. Cryptophyceae**	
Stauropsis Meunier	29	*Chroomonas* Hansgirg	9
Staurosira (Ehrenberg) Williams & Round	29	*Cryptomonas* Ehrenberg	2
Stellarima Hasle & Sims	4		
Stenopterobia de Brébisson ex Van Heurck	13	**7. Dinophyceae**	
Stephanodiscus Ehrenberg	4	*Alexandrium* Halim	3
Stephanopyxis (Ehrenberg) Ehrenberg	5	*Amphidinium* Claparède et Lachmann	3
Stictodiscus Greville	4	*Amphisolenia* Stein	4
Striatella Agardh	29	*Balechina* Loeblich J & Loeblich III	2
Surirella Turpin	11	*Blepharocysta* Ehrenberg	1
Synedra Ehrenberg	10	*Ptychodiscus* Stein	2
		(continued)	

Table I: (continued)

Genera	Shape code	Genera	Shape code
Synedrosphenia (Peragallo) Azpeitia	21	*Pyrocystis* Murray ex Haeckel	3
Tabellaria Ehrenberg	20	*Pyrophacus* Stein	3
Cladopyxis Stein	1	*Scrippsiella* Balech ex Loeblich III	9
Dinophysis Ehrenberg	3	*Schuettiella* Balech	8
Diplopelta Stein ex Jörgensen	3	*Spiraulax* Kofoid	8
Diplopsalis Bergh	9	*Symbiodinium* Freudenthal	2
Dissodinium Pascher	3	*Triposolenia* Kofoid	27
Gambierdiscus Adachi & Fukuyo	3	*Centrodinium* Kofoid	8
Gloeodinium Klebs	3	*Ceratium* Schrank	25
Goniodoma Stein	1	*Ceratocorys* Stein	26
Gonyaulax Diesing	8		
		8. Euglenophyceae	
Gymnodinium Stein	3	*Euglena* Ehrenberg	22
Gyrodinium Kofoid & Swezy	3	*Eutreptia* Perty	22
Heteraulacus Diesing	3		
Heterodinium Kofoid	8	**9. Prasinophyceae**	
Histioneis Stein	3	*Halosphaera* Schmitz	1
Karenia Daugbjerg, Hansen, Larsen, Moestrup	3	*Mantoniella* Desikachary	2
		Micromonas Manton & Parke	2
Kofoidinium Pavillard	1	*Nephroselmis* Stein	1
Lingulodinium Dodge	3	*Pyramimonas* Schmarda	7
Noctiluca Suriray	1		
Ornithocercus Stein	26		
Ostreopsis Schmidt	3	**10. Chlorophyceae**	
Oxytoxum Stein	2	*Actinastrum* Lagerheim	2
Peridiniopsis Lemmermann	3	*Ankistrodesmus* Cord	16
Peridinium Ehrenberg	3	*Brachiomonas* Bohlin	8
Phalacroma Stein	3	*Carteria* Diesing	1
Podolampas Stein	7	*Chlamydomonas* Ehrenberg	1
Polykrikos Bütschli	3	*Dunaliella* Teodoresco	2
Preperidiunium Mangin	3	*Pediastrum* Meyen	11
Prorocentrum Ehrenberg	3	*Scenedesmus* Meyen	2
Protoperidinium Bergh	8	*Tetraëdron* Kützing	10

we used the linear dimensions for length, width and height instead of apical axis, transapical axis and perval-var axis. For example, when phytoplankton samples were observed under the light microscope, in most circumstances, the length (may be the pervalvar axis in some diatoms, e.g. *Leptocylindrus* spp.) and width were measured, then the cell volume and surface area were calculated from the geometric models discussed in this paper. The models were checked with a set of phytoplankton counter data and a Visual Basic for Applications (VBA) program was written in Microsoft Excel for calculations.
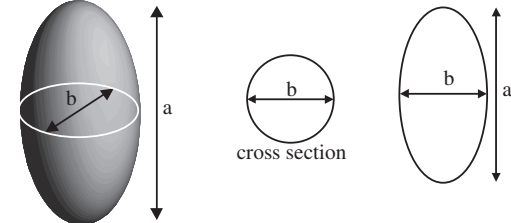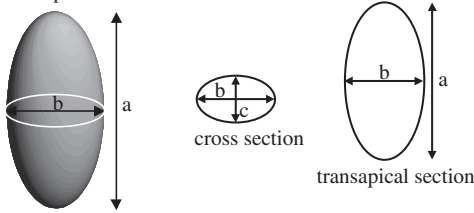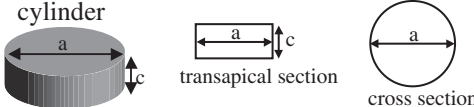
METHOD

Phytoplankton samples from sample sites covering most of China's seas (with samples collected from the first comprehensive investigation in 1958 up to now) were selected and analysed using a light microscope. Net samples were collected with a standard net III (76 μm mesh size, simple conical tow net, which is a standard phytoplankton tool used in China) and a vertical haul was made from just off the bottom to the surface. These samples were preserved in 2 or 5% neutral formaldehyde (final concentration) in glass or polyethylene bottles. Samples were observed with

an Olympus BH-2 microscope at × 200, × 400 or × 1000 magnification in a phytoplankton counting chamber (a standard tool used in China fabricated in our laboratory, 0.25 ml, similar to a Palmer–Maloney chamber) and identified to species level (Yamaji, 1991; Tomas, 1997). Water samples were preserved initially in 250 ml polyethylene bottles containing 1% Lugol's iodine solution and ultimately the samples were preserved in 1% neutral formaldehyde (final concentration). Twenty-five millilitres of preserved sample were left for >24 h in settling chambers and then analysed with an American Optical Ltd inverted microscope at × 200, × 200 or × 640 magnification (Utermöhl, 1958) to identify phytoplankton to species level (Yamaji, 1991; Tomas, 1997). The scale bar for the microscopic ocular was calibrated using a

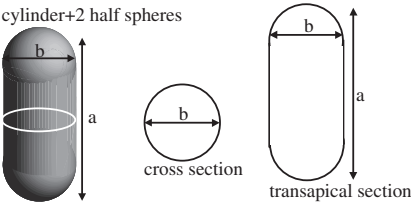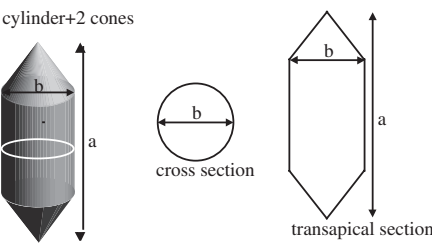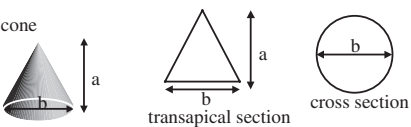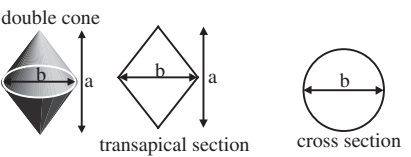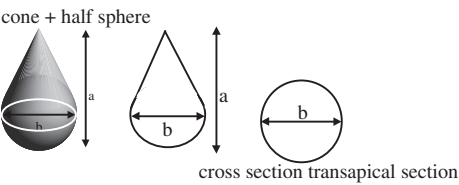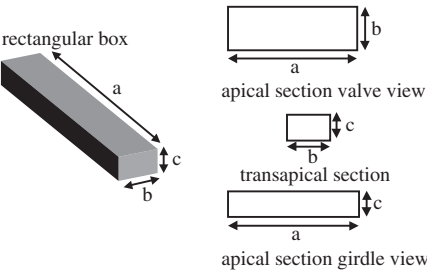standard scale bar (S22-StageMic; Graticules Ltd, UK) mounted on the microscopic objective.

Linear dimensions were measured according to Table II or by obtaining taxonomic information and searching the shape code in Table I. In most cases, it was possible to determine the length and width of the target cell. As the cell settles on the base plate on the posture of synthetic effect of several forces, such as gravitation and buoyancy, the length may not always be the apical axis. The individual analysing the sample need not consider the morphological information when using this set of models, thus the applicability will be improved in the models. The height of the target cell can be measured after rolling the cell by gently touching the coverslip with a pin-like object under routine examination by light microscope.

Table II: Geometric shapes and equations for the calculation of biovolume and surface area

Shape code	Simulated shape	Volume (V) and surface area (A) model
1-H	sphere cross section	$V = \frac{\pi}{6} \cdot a^3$ $A = \pi \cdot a^2$
2-H	prolate spheroid cross section	$V = \frac{\pi}{6} \cdot b^2 \cdot a$ $A = \frac{\pi \cdot b}{2}\left(b + \frac{a^2}{\sqrt{a^2 - b^2}}\sin^{-1}\frac{\sqrt{a^2 - b^2}}{a}\right)$
3-H	ellipsoid cross section transapical section	$V = \frac{\pi}{6} \cdot a \cdot b \cdot c$ $A \approx \frac{\pi}{4} \cdot (b + c) \cdot$ $\left[\left(\frac{b+c}{2}\right) + \frac{2a^2}{\sqrt{4a^2 - (b+c)^2}}\sin^{-1}\frac{\sqrt{4a^2 - (b+c)^2}}{2a}\right]$
4-H	cylinder transapical section cross section	$V = \frac{\pi}{4} \cdot a^2 \cdot c$ $A = \pi \cdot a \cdot \left(\frac{a}{2} + c\right)$
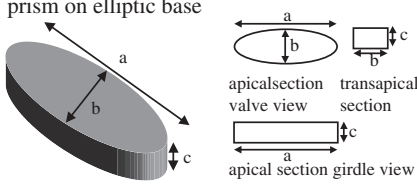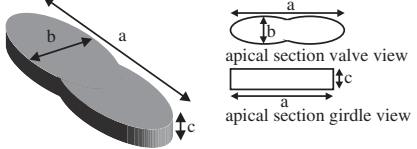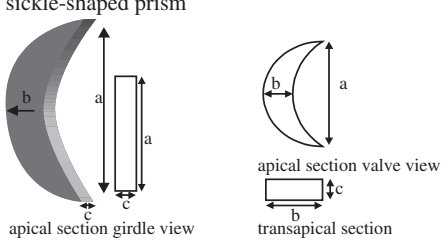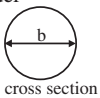
(continued)

Table II: (continued)

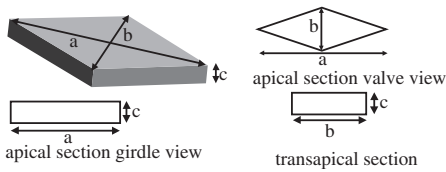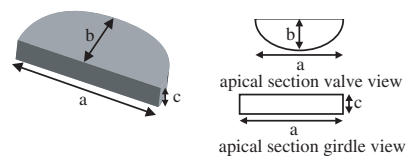| Shape code	Simulated shape	Volume (*V*) and surface area (*A*) model
5-H	cylinder+2 half spheres cross section · transapical section	$V = \pi \cdot b^2 \cdot \left(\dfrac{a}{4} - \dfrac{b}{12}\right)$ $A = \pi \cdot a \cdot b$
6-H	cylinder+2 cones cross section · transapical section	Suppose the height of cones is half of b : $V = \dfrac{\pi}{4} \cdot b^2 \cdot \left(a - \dfrac{b}{3}\right)$ $A = \pi \cdot b \cdot \left(a - \dfrac{4 - \sqrt{3}}{4} b\right)$
7-H	cone transapical section · cross section	$V = \dfrac{\pi}{12} \cdot a \cdot b^2$ $A = \dfrac{\pi}{4} \cdot b \cdot \left(b + \sqrt{4a^2 + b^2}\right)$
8-H	double cone transapical section · cross section	$V = \dfrac{\pi}{12} \cdot a \cdot b^2$ $A = \dfrac{\pi}{2} \cdot b \cdot \sqrt{a^2 + b^2}$
9-H	cone + half sphere cross section transapical section	$V = \dfrac{\pi}{4} \cdot a \cdot b^2$ $A = \dfrac{\pi}{2} \cdot b^2 \cdot \left(b + \sqrt{\dfrac{2a^2 - ab + b^2}{2}}\right)$
10-H	rectangular box apical section valve view transapical section apical section girdle view	$V = a \cdot b \cdot c$ $A = 2 \cdot a \cdot b + 2 \cdot b \cdot c + 2 \cdot a \cdot c$

(continued)

Table II: (continued)

Shape code	Simulated shape	Volume (*V*) and surface area (*A*) model
11-H	prism on elliptic base	$V = \frac{\pi}{4} \cdot a \cdot b \cdot c$ $A = \frac{\pi}{2} \cdot (a \cdot b + b \cdot c + a \cdot c)$
12-H	elliptic prism with transapical constriction	$V \approx \frac{\pi}{4} \cdot a \cdot b \cdot c$ $A \approx \frac{\pi}{2} \cdot (a \cdot b + b \cdot c + a \cdot c)$
13-H	prism on parallelogram-base	$V = \frac{1}{2} \cdot a \cdot b \cdot c$ $A = a \cdot b + \frac{\sqrt{a^2 + b^2}}{4} \cdot c$
14-H	half-elliptic prism	$V = \frac{\pi}{4} \cdot a \cdot b \cdot c$ $A = \frac{\pi}{4} \cdot (a \cdot b + b \cdot c + a \cdot c) + a \cdot c$
15-H	sickle-shaped prism	$V \approx \frac{\pi}{4} \cdot a \cdot b \cdot c$ $A \approx \frac{\pi}{4} \cdot (a \cdot b + b \cdot c + a \cdot c) + a \cdot c$
16-H	sickle-shaped cylinder	$V \approx \frac{\pi}{6} \cdot a \cdot b^2$ $A \approx \frac{\pi}{2} \cdot b \cdot \sqrt{a^2 + b^2}$
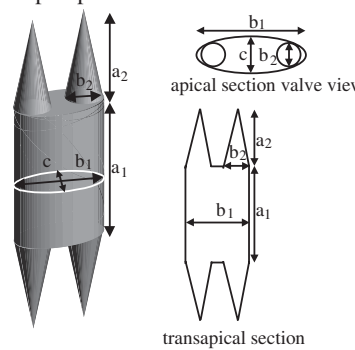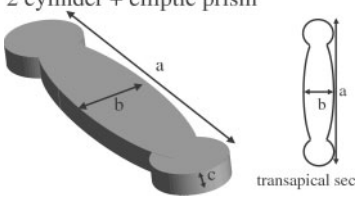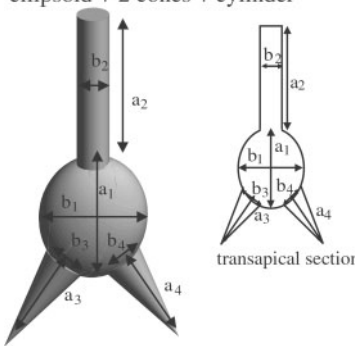
For 11-H: apical section valve view, transapical section, apical section girdle view.

For 12-H: apical section valve view, apical section girdle view.

For 13-H: apical section valve view, apical section girdle view, transapical section.

For 14-H: apical section valve view, apical section girdle view.

For 15-H: apical section valve view, apical section girdle view, transapical section.

For 16-H: cross section.

Table II: *(continued)*

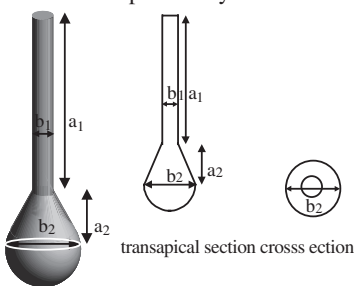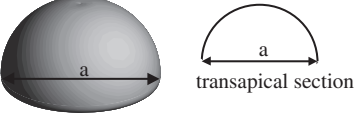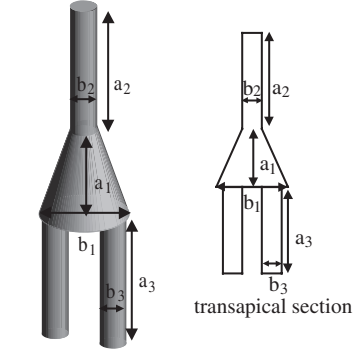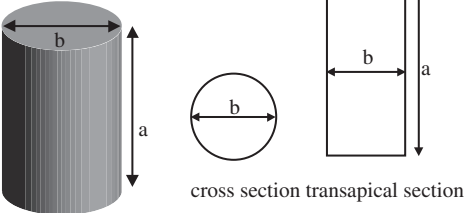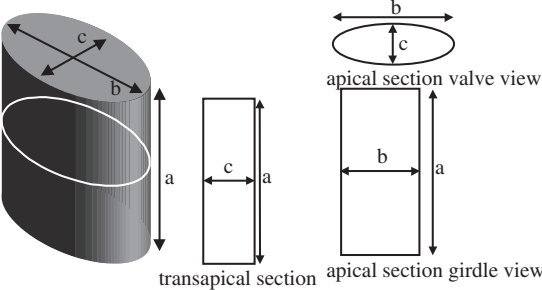| Shape code	Simulated shape	Volume (*V*) and surface area (*A*) model
17-H	cymbelloid apical section / transapical section	$V = \dfrac{2}{3} \cdot a \cdot c^2 \cdot \operatorname{asin}\left(\dfrac{b}{2c}\right)$ $A = \dfrac{\pi}{2} \cdot a \cdot c + b \cdot \left[c + \dfrac{a^2}{2\sqrt{a^2 - 4c^2}} \cdot \sin^{-1}\left(\dfrac{\sqrt{a^2 - 4c^2}}{a}\right)\right]$
18-H	prism on triangle-base transapical section	$V = \dfrac{\sqrt{3}}{4} \cdot c \cdot a^2$ $A = 3a \cdot c + \dfrac{\sqrt{3}}{2} \cdot a^2$
19-H	pyramid transapical section / apical section valve view	$V = \dfrac{1}{6} \cdot a^2 \cdot c$ $A = \dfrac{1}{2} \cdot a^2 + a \cdot \sqrt{a^2 + 8c^2}$
20-H	elliptic prism with transapical inflation apical section valve view / apical section girdle view / transapical section	$V \approx \dfrac{\pi}{4} \cdot a \cdot b \cdot c$ $A \approx \dfrac{\pi}{2} \cdot (a \cdot b + b \cdot c + a \cdot c)$
21-H	gomphonemoid apical section girdle view / transapical view from base pole / apical section valve view	$V \approx \dfrac{a \cdot b}{4} \cdot \left[a + \left(\dfrac{\pi}{4} - 1\right) \cdot b\right] \cdot \operatorname{asin}\left(\dfrac{c}{2a}\right)$ $A \approx \dfrac{b}{2} \cdot \left(2a + \pi \cdot a \cdot \operatorname{asin}\left(\dfrac{c}{2a}\right) + \left(\dfrac{\pi}{2} - 2\right) \cdot b\right)$

(continued)

Table II: (continued)

Shape code	Simulated shape	Volume (V) and surface area (A) model
22-SL	cone + half sphere + cylinder transapical section cross section	$V = \dfrac{\pi}{3} \cdot (a_1 + a_2) \cdot b_1^2 + \dfrac{\pi}{4} \cdot (a_2 + b_2) \cdot b_2^2 + \dfrac{\pi}{12} \cdot a_2 \cdot b_1 \cdot b_2$ $A = \pi \cdot a_1 \cdot b_1 + \dfrac{\pi}{4} \cdot b_1^2 + \dfrac{\pi}{2} \cdot b_2^2 + \dfrac{\pi}{2} \cdot b_2^2 \cdot \sqrt{\left(\dfrac{a_1}{b_1}\right)^2 + \dfrac{1}{4}}$ $\qquad - \dfrac{\pi}{2} \cdot b_1 \cdot \sqrt{\left(\dfrac{a_1 \cdot b_2}{b_1} - a_1\right)^2 + \dfrac{b_1^2}{4}}$
23-SL	elliptic prism + 4 cone apical section valve view transapical section	$V = \dfrac{\pi}{4} \cdot a_1 \cdot b_1 \cdot c_1 + \dfrac{\pi}{3} \cdot a_2 \cdot b_2^2$ $A = \dfrac{\pi}{2} \cdot a_1 \cdot b_1 + \dfrac{\pi}{2} \cdot b_1 \cdot c_1 + \dfrac{\pi}{2} \cdot a_1 \cdot c_1 + \pi \cdot b_2 \cdot \left(\sqrt{4a_2^2 + b_2^2} - b_2\right)$
24-SL	2 cylinder + elliptic prism transapical section	$V \approx \dfrac{\pi}{4} \cdot a \cdot b \cdot c$ $A \approx \dfrac{\pi}{2} \cdot (a \cdot b + b \cdot c + a \cdot c)$
25-SL	ellipsoid + 2 cones + cylinder transapical section	Suppose : $b_2 = b_3 = b_4$ $V = \dfrac{\pi}{4} \cdot a_2 \cdot b_2^2 + \dfrac{\pi}{12} \cdot (a_3 + a_4) \cdot b_2^2 + \dfrac{\pi}{6} \cdot a_1 \cdot b_1 \cdot b_2$ $A \approx \dfrac{\pi}{4} \cdot (b_1 + b_2) \cdot \left[\dfrac{b_1 + b_2}{2} + \dfrac{a_1^2}{\sqrt{a_1^2 - \left(\frac{b_1+b_2}{2}\right)^2}} \cdot \sin^{-1} \dfrac{\sqrt{a_1^2 - \left(\frac{b_1+b_2}{2}\right)^2}}{a_1}\right]$ $\qquad + \dfrac{\pi}{2} \cdot b_2 \cdot \left(2a_2 + \sqrt{a_3^2 + \dfrac{b_2^2}{4}} + \sqrt{a_4^2 + \dfrac{b_2^2}{4}} - b_2\right)$

(continued)

Table II: (continued)

Shape code	Simulated shape	Volume (V) and surface area (A) model
26-SL	half sphere transapical section	$V = \dfrac{\pi}{12} \cdot a^3$ $A = \dfrac{3\pi}{4} \cdot a^2$
27-SL	cone + 3 cylinder transapical section	$V = \dfrac{\pi}{4} \cdot a_2 \cdot b_2^2 + \dfrac{\pi}{2} \cdot a_3 \cdot b_3^2 + \dfrac{\pi}{12} \cdot a_1 \cdot (b_1^2 + b_1 \cdot b_2 + b_2^2)$ $A = \dfrac{\pi}{2} \cdot (b_1 + b_2) \cdot \sqrt{a_1^2 + \left(\dfrac{b_1 - b_2}{2}\right)^2} + \dfrac{\pi}{4} \cdot (b_1^2 + b_2^2)$ $\qquad + 2\pi \cdot (a_2 \cdot b_2 + a_3 \cdot b_3)$
28-H	cylinder girdle view cross section transapical section	$V = \dfrac{\pi}{4} \cdot b^2 \cdot a$ $A = \pi \cdot b \cdot \left(\dfrac{b}{2} + a\right)$
29-H	prism on elliptic base girdle view transapical section apical section girdle view	$V = \dfrac{\pi}{4} \cdot a \cdot b \cdot c$ $A = \dfrac{\pi}{2} \cdot (a \cdot b + b \cdot c + a \cdot c)$

(continued)

Table II: (continued)

Shape code	Simulated shape	Volume (*V*) and surface area (*A*) model
30-H	prism on triangle-base girdle view a apical section valve view transapical section	$V = \frac{\sqrt{3}}{4} \cdot a \cdot b^2$ $A = 3a \cdot b + \frac{\sqrt{3}}{2} \cdot b^2$
31-SL	box + elliptic prism transapical section	$V \approx c \cdot \left(a_1 \cdot b_1 + \frac{\pi}{4} \cdot a_2 \cdot b_2 \right)$ $A \approx c \cdot \left(2a_1 + b_1 + \frac{\pi}{2} \cdot a_2 + \frac{\pi}{2} \cdot b_2 \right) + 2a_1 \cdot b_1 + \frac{\pi}{2} \cdot a_2 \cdot b_2$

Simulated shapes were given by a three-dimensional image with a cross-section view or a transapical section view. In the shape code column, H = models from Hillebrand *et al.* (Hillebrand *et al.*, 1999), amended by ourselves; SL = models from Sun & Liu in this paper; *V* = volume; *A* = surface area; *a* = length; *b* = width; *c* = height. Other symbols are marked in the table.

Twenty or more individual cells should be measured to avoid biasing results (Sournia, 1978; Hillebrand *et al.*, 1999). The information on taxa and linear dimensions were then input into a Microsoft Excel worksheet; cell and community biovolume and surface areas were calculated by a VBA program which compiled data according to the shape code in Table I and the equation in Table II. History samples from which the cell abundance and community information to species level have been derived can also be converted from cell counts to biovolume and surface area. When linear dimensions of 20 typical cells in the sample were measured, individual cells of chain-forming species were measured and calculated. Software enabling these calculations is available from the first author, or at http://www.ouc.edu.cn/csmxy/sunjun/biovolume.htm.

RESULTS AND DISCUSSION

Measurement of phytoplankton cell height

Measuring the height of phytoplankton cells under the microscope can be difficult for some species. The algal cell usually keeps a definite position on the slide when the centre of gravity is low, making it difficult to measure the cell height. In most instances, an algal species will keep a fixed position, but on rare occasions the side view of the cell is visible, providing the opportunity to measure the height. If the cell is rotated, it will increase the chances of getting a side view. Using a pin-like object to tip the coverslip, algal cells will roll with the movement of the surrounding medium.

Usually it is not possible to rotate the cell using a pin in order to measure the cell height, either when the sample is examined by the Utermöhl method or when special counting slides such as Sedgwick–Rafter or Palmer–Maloney slides are used. There are two ways to solve the problem: one is to concentrate the sample after observation and follow up with a standard compound microscope; the other is to estimate the height from the width of the cell, because the height of small algal cells is usually approximately equal to the width. Verity *et al.* also pointed out that there is little variation between the depth and width of nanoplankton cells (Verity *et al.*, 1992). However, as Hillebrand *et al.* (Hillebrand *et al.*, 1999) suggest, the height of large cells should be measured.

Error sources in the models

For each genus, the error sources within these models come from the choice of geometric shapes assigned to the algal cell, in addition to the accuracy of measurement and consequent estimation of biovolume.

The selection of geometric shapes in this model was similar to Hillebrand's model (Hillebrand *et al.*, 1999). It was based on an assumption of similar shapes within each genus. In general, this principle applies, but there are some exceptions within genera, as pointed out by Hillebrand *et al.* (Hillebrand *et al.*, 1999). The main distinguishing feature between these two models is that some geometric shapes were divided into two similar models for convenience of measurement, each one being the side view of the opposite one, such as 'prism on elliptic base' and 'prism on elliptic base girdle view' (cf. Table II). Meanwhile, six additional geometric shapes were assigned to additional morphologically complex genera.

The measurement procedure can potentially be the largest error source when estimating biovolume if the sampler does not follow the standard protocol accurately. The scale bar must be calibrated for each magnification. Light halos affect the measurement of small-sized cells (Montagne *et al.*, 1994), but can be overcome by increasing the magnification of the microscope.

Between the initial field sampling and final interpretation of data, there are several potential sources of bias or variability. They include initial sampling methods, preservation (primary samples), subsampling (including concentration or dilution), counting use of tertiary subsamples, or random field selection, and statistical analyses. Some of these can be minimized or eliminated by following a strictly standardized procedure (Sournia, 1978; Hallegraeff *et al.*, 1995).

It is not possible to measure every cell during routine analysis. Subsamples for line dimension measurement should consider phytoplankton assemblages. For each phytoplankton assemblage, at least 25 randomly selected cells of each species should be measured (Smayda, 1978), and the mean biovolume should be calculated from the mean value of these individual cell biovolumes. Hillebrand *et al.* propose that biovolume should be calculated from the mean of measured linear dimensions, not as a mean of a set of individually calculated biovolumes (Hillebrand *et al.*, 1999). When the two methods for mean biovolume calculation were compared, we found that although the latter method usually underestimated the variability, its trend has better agreement with increased measurements (Figure 1). Thus, the mean measured linear dimension can be used to calculate biovolume in routine analysis. Although, under most circumstances, the standard error (SE) is < 5% of the mean biovolume after the measurement of 10 cells (cf. Figure 1), we suggest that taking as many measurements as possible is better.

Comparison with other models

A comparison between this study and the other three models, Hansen (Hansen, 1992), HELCOM (Helsinki Commission, 2000) and BIOVOL (Kirschtel, 1992), is shown in Figure 2. Five typical species were assigned to five different geometric shapes with a length/width ratio from 1.2 to 25. Sample measurements were conducted under the microscope as described previously. Compared with these models, Hansen's model underestimated the volume and the BIOVOL model overestimated the biovolume. The HELCOM model had similar results to our study. However, most results have a SE of not more than 30%. With the exception of *Ceratium furca*, the calculation equations of the other four species in this study were equal to the Hillebrand *et al.* model (Hillebrand *et al.*, 1999). Hillebrand *et al.* (Hillebrand *et al.*, 1999) also compared their results with Edler's model (Edler, 1979), Rott's model (Rott, 1981) and Kovala–Larrance's model (Kovala and Larrance, 1966). They pointed out that there were some genera without a geometric model for calculating biovolume. In each model mentioned in this paper, including this study, none can give every phytoplankton species/genera a geometric model for calculating biovolume. Because of the diversity of phytoplankton morphology, it is impossible to calculate biovolume according to a set of geometric models, but all the models determine biovolume by simulation. It is important to focus on how to attain more accurate and available data when we choose appropriate models to calculate biovolume. Thus, for resolving a specific problem we can use different biovolume models. For example, Young and Ziveri use a cubic function, $V = K_s \times l^\beta$, to calculate coccolithophorids (Young and Ziveri, 2000). They assigned a specific shape constant, K_s, to a definite coccolithophorid species, thus they can get a more accurate value of biovolume for the species. If a phytoplankton assemblage is dominated by a microalga that has a more complex geometric shape, such as *C. furca*, it is important to produce a more complex geometric model or employ the models mentioned above to calculate this particular species.

Related ecological parameters

Biovolume and surface area calculations for phytoplankton cells are important for many related ecological parameters (Malone, 1980; Sournia, 1981; Chisholm, 1992), such as biomass, growth, photosynthesis, respiration, assimilation, sinking, grazing, etc. Most relationships between these parameters and biovolume follow the allometric theory, i.e. $R = a \times V^b$, where R is a specific
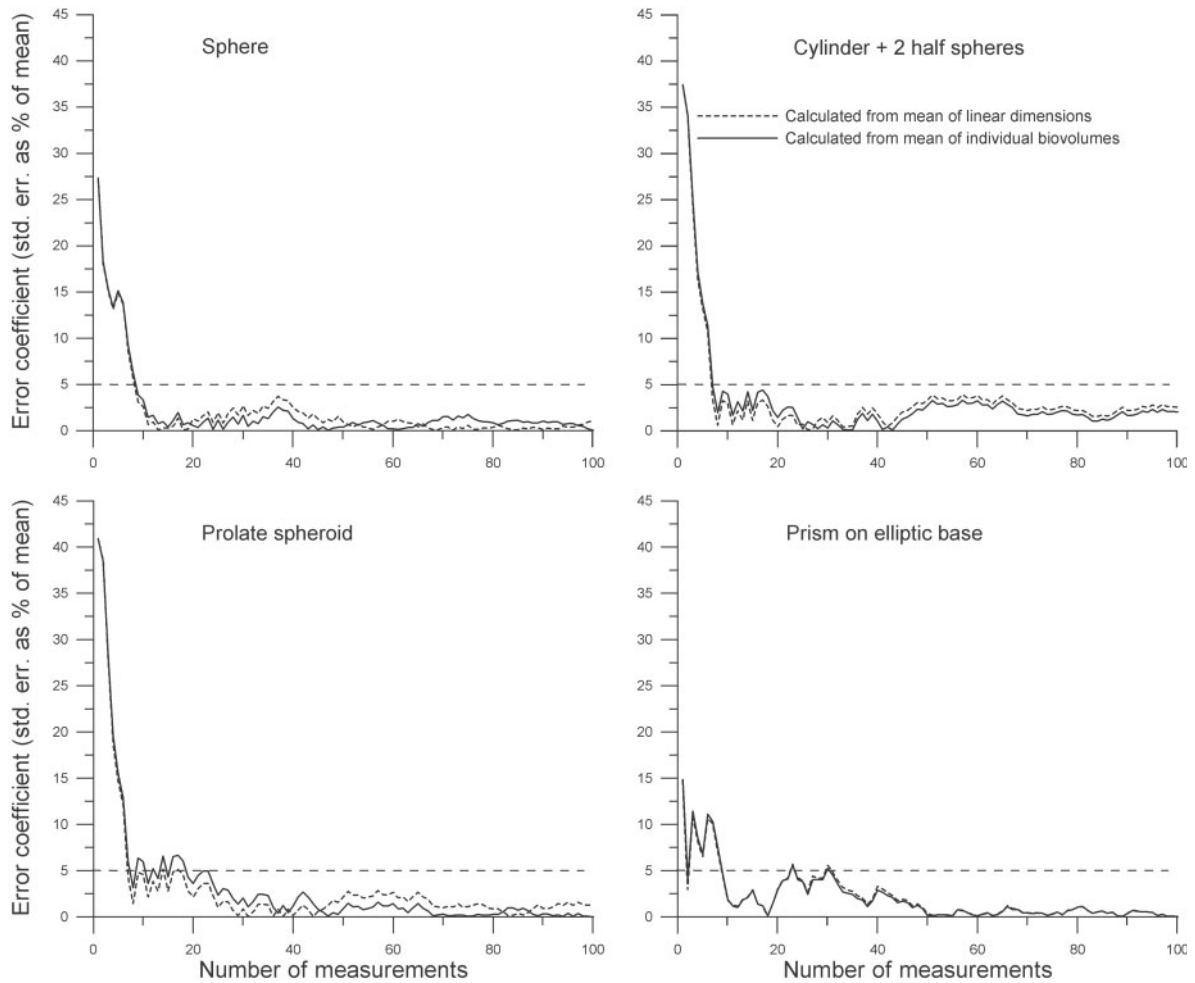
Fig. 1. Comparison of the mean biovolume of four species calculated from the mean of the linear dimension (dashed line) or the mean of individual biovolumes (solid line).
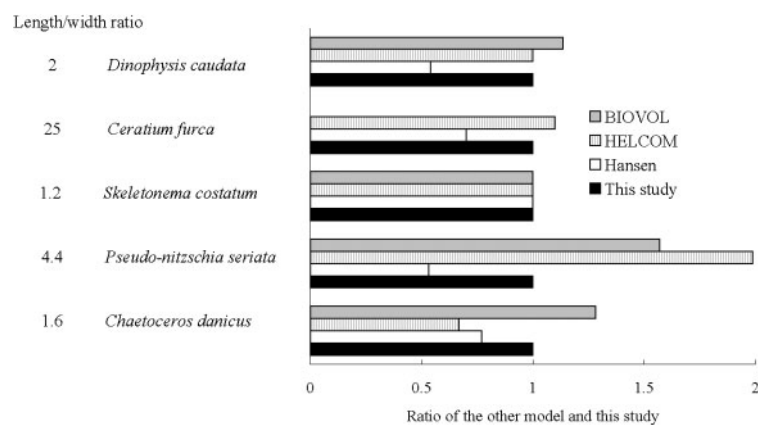
Fig. 2. Comparison of calculated biovolume by four models for five typical phytoplankton species.

rate process or biomass, V is biovolume, and a and b are constants. So the biovolume and surface area of phytoplankton cells are used for conversion of cell counts into many related parameters. Although this procedure is complex and tedious, the conversion parameters provide the opportunity of differentiating between the con-

tribution of different taxonomic groups which cannot be calculated accurately in 'bulk measurement'.

In these biovolume-related parameters, carbon conversion is obviously important to phytoplankton studies, and is becoming a routine quantity derived from phytoplankton sample analyses. Several relationships between carbon and biovolume have been established in the literature (Mullin *et al.*, 1966; Strathmann, 1967; Eppley *et al.*, 1970; Taguchi, 1976; Rocha and Duncan, 1985; Verity *et al.*, 1992; Montagne *et al.*, 1994; Menden-Deuer and Lessard, 2000). The different phytoplankton assemblages have their own special carbon–biovolume relationship, but this measurement has not been carried out in the China Sea waters until now. Following the calculation of biovolume for 87 commonly found phytoplankton species in China Sea waters, Sun *et al.* (Sun *et al.*, 2000a) compared four carbon–biovolume relationships (Mullin *et al.*, 1966; Strathmann, 1967; Eppley *et al.*, 1970; Taguchi, 1976) for carbon estimation of net phytoplankton, and proposed using Eppley's method (Eppley *et al.*, 1970) for carbon conversion in China Sea waters.

Model applications in China

There are few biovolume studies on phytoplankton in China (Sun *et al.*, 2000a,b,c 1980). In these studies, Jiaozhou Bay was chosen as a case study area, and phytoplankton cell biovolume was calculated for each species by assigning one or several combinations of regular geometric shapes. This is not easily done as we required to consider each species' morphological information. The new model, as described above, was established at the end of 1999. According to the convenient feature of inputting data in Microsoft Excel, we compiled a VBA program for this model. This model was tested using the conversion carbon estimates from elsewhere (Sun *et al.*, 2001).

In conclusion, the geometric model for estimating phytoplankton cell biovolume is applicable in China and easier to use in routine phytoplankton analyses. It provides taxonomic information while calculating biovolume-related parameters. Its application should be extended to other regions, and should be attempted in many other related fields, such as historical data assimilations, studies on carbon flux at the species level, studies on biovolume and surface area relationship with related parameters, etc.

ACKNOWLEDGEMENTS

REFERENCES

Baltic Marine Environmental Protection Commission–Helsinki Commission (1988) *Guidelines for the Baltic Monitoring Programme for the Third Stage: Part D. Biological Determinants. Baltic Sea Environmental Proceedings No. 27 D.* BMEPC-HC.

Boyd, C. M. and Johnson, C. W. (1995) Precision of size determination of resistive electronic particle counters. *J. Plankton Res.*, **17**, 41–58.

Brown, L. M., Gargantini, I., Brown, D. J., Atkinson, H. J., Govindarajan, J. and Vanlerberghe, G. C. (1989) Computer-based image analysis for the automated counting and morphological description of microalgae in culture. *J. Appl. Phycol.*, **1**, 211–225.

Chisholm, S. W. (1992) Phytoplankton size. In Falkowski, P. G. and Woodhead, A. D. (eds), *Primary Productivity and Biogeochemical Cycles in the Sea.* Plenum Press, New York, pp. 213–237.

Cunningham, A. and Buonnacorsi, C. A. (1992) Narrow-angle forward light scattering from individual algal cells: implications for size and shape discrimination in flow cytometry. *J. Plankton Res.*, **14**, 223–234.

Edler, L. (ed.) (1979) *Phytoplankton and Chlorophyll: Recommendations on Methods for Marine Biological Studies in the Baltic Sea. Baltic Marine Biologists Publication No. 5.*

Eppley, R. W., Reid, F. M. H. and Strickland, J. D. H. (1970) Estimates of phytoplankton crop size, growth rate and primary production. *Bull. Scripps Inst. Oceanogr.*, **17**, 33–42.

Estep, K. W., MacIntyre, F., Hjorleifsson, E. and Sieburth, J. M. (1986) MacImage: a user friendly image-analysis system for the accurate mensuration of marine organisms. *Mar. Ecol. Prog. Ser.*, **33**, 243–253.

Gordon, R. (1974) A tutorial on ART (algebraic reconstruction techniques). *IEEE Trans. Nucl. Sci.*, **21**, 78–93.

Hallegraeff, G. M., Anderson, D. M. and Cembella, A. D. (eds) (1995) *Manual on Harmful Marine Microalgae. IOC Manuals and Guides No. 33.* UNESCO, Paris.

Hansen, G. (1992) Biomasseberegninger. In Thomsen, H. A. (ed.), *Plankton i de indre danske farvande.* Havforskning fra Miljøstyrelsen, Miljøministeriet, pp. 20–34.

Hastings, J. W., Sweeney, B. M. and Mullin, M. M. (1962) Counting and sizing of unicellular marine organisms. *Ann. N. Y. Acad. Sci.*, **99**, 180–289.

Helsinki, Commission (2000) *Phytoplankton Species Composition, Abundance and Biomass.* HELCOM. Available at http://sea.helcom.fi/manual/anxc6.html

Hillebrand, H. (1997) Response of epilithic microphytobenthos of the Western Baltic Sea to *in situ* experiments with nutrient enrichment. *Mar. Ecol. Prog. Ser.*, **160**, 35–46.

Hillebrand, H., Dürselen, C. D., Kirschtel, D., Pollingher, D. and Zohary, T. (1999) Biovolume calculation for pelagic and benthic microalgae. *J. Phycol.*, **35**, 403–424.

Kirschtel, D. B. (1992) Calculating the biovolume and surface area of irregularly shaped diatoms. *Bull. N. Am. Benth. Soc.*, **9**, 159.

Kononen, K., Forsskaehl, M., Huttunen, M., Sandell, M. and Viljamaa, M. H. (1984) Practical problems encountered in phytoplankton cell volume calculations using the BMB recommendation in the Gulf of Finland. *Limnologica*, **15**, 605–614.

Kovala, P. E and Larrance, J. P. (1966) *Computation of Phytoplankton Cell Numbers, Cell Volume, Cell Surface Area and Plasma Volume per Litre, from Microscopical Counts. Special Report, Vol. 38*. University of Washington, Seattle, WA, pp. 1–91.

Krambeck, C., Krambeck, H. J. and Overbeck, J. (1981) Microcomputer-assisted biomass determination of plankton bacteria on scanning electron micrographs. *Appl. Environ. Microbiol.*, **42**, 142–149.

Kramer, K. J. M., Warwick, R. M. and Brockmann, U. H. (1992) *Manual of Sampling and Analytical Procedures for Tidal Estuaries*. Electronic Publishing Centre, TNO, Delft.

Kuuppo, P. (1994) Annual variation in the abundance and size of heterotrophic nanoflagellates on the SW coast of Finland, the Baltic sea. *J. Plankton Res.*, **16**, 1525–1542.

Malone, T. C. (1980) Algal size. In Morris, I. (ed.), *The Physiological Ecology of Phytoplankton*. University of California Press, California, pp. 433–463.

Maloney, T. E., Donovan, E. J., Jr and Robinson, E. L. (1962) Determination of numbers and sizes of algal cells with an electronic particle counter. *Phycologia*, **2**, 1–8.

Menden-Deuer, S. and Lessard, E. J. (2000) Carbon to volume relationships for dinoflagellates, diatoms, and other protist plankton. *Limnol. Oceanogr.*, **45**, 569–579.

Montagne, D. J. S., Berges, J. A., Harrison, P. J. and Taylor, F. J. (1994) Estimationg carbon, nitrogen, protein, and chlorophyll *a* from volume in marine phytoplankton. *Limnol. Oceanogr.*, **39**, 1044–1060.

Mullin, M. M., Sloan, P. R. and Eppley, R. W. (1966) Relationship between carbon content, cell volume, and area in phytoplankton. *Limnol. Oceanogr.*, **11**, 307–311.

Olson, R. J., Vaulot, D. and Chisholm, S. W. (1985) Marine phytoplankton distributions measured using shipboard flow cytometry. *Deep-Sea Res.*, **32**, 1273–1280.

Rocha, O. and Duncan, A. (1985) The relationship between cell carbon and cell volume in freshwater algal species used in zooplankton studies. *J. Plankton Res.*, **7**, 279–294.

Rott, E. (1981) Some results from phytoplankton counting intercalibrations. *Schweiz. Z. Hydrol.*, **43**, 34–62.

Sicko-Goad, L., Stoermer, E. F. and Ladewski, B. G. (1977) A morphometric method for correcting phytoplankton cell volume estimates. *Protoplasma*, **93**, 147–163.

Sieracki, C. K., Sieracki, M. E. and Yentsch, C. M. (1998) An imaging-in-flow system for automated analysis for marine microplankton. *Mar. Ecol. Prog. Ser.*, **168**, 285–296.

Smayda, T. J. (1978) From phytoplankton to biomass. In Sournia, A. (ed.), *Phytoplankton Manual. Monographs on Oceanographic Methodology 6*. UNESCO, Paris, pp. 273–279.

Snoeijs, P. (1994) Distribution of epiphytic diatom species composition, diversity and biomass on different macroalgal hosts along seasonal and salinity gradients in the Baltic Sea. *Diatom Res.*, **9**, 189–211.

Sommer, U. (1994) Are marine diatoms favoured by high Si:N ratio? *Mar. Ecol. Prog. Ser.*, **115**, 309–315.

Sommer, U. (1995) An experimental test of the intermediate disturbance hypothesis using cultures of marine phytoplankton. *Limnol. Oceanogr.*, **40**, 1271–1277.

Sournia, A. (ed.) (1978) *Phytoplankton Manual. Monographs on Oceanographic Methodology 6*. UNESCO, Paris.

Sournia, A. (1981) Morphological base of competition and succession. *Can. Bull. Fish. Aquat. Sci.*, **210**, 339–346.

Steen, H. B. (1990) Characters of flow cytometers. In Melamed, M. R., Lindmo, T. and Mendelsohn, M. L. (eds), *Flow Cytometry and Sorting*, 2nd edn. Wiley-Liss, New York, pp. 11–25.

Strathman, R. R. (1967) Estimating the organic carbon content of phytoplankton from cell volume or plasma volume. *Limnol. Oceanogr.*, **12**, 411–418.

Sun, J., Liu, D. Y. and Qian, S. B. (2000a) Estimating biomass of phytoplankton in the Jiaozhou Bay, I. Phytoplankton biomass estimated from cell volume and plasma volume. *Acta Oceanol. Sin.*, **19**, 19–31.

Sun, J., Liu, D. Y. and Qian, S. B. (2000b) Study on phytoplankton biomass, II. Net-phytoplankton measurement biomass estimated from cell volume in the Jiaozhou Bay. *Acta Oceanol. Sin.*, **22**, 102–109 (in Chinese).

Sun, J., Liu, D. Y. and Qian, S. B. (2000c) Study on phytoplankton biomass, III. Estimated bulk measurement biomass of phytoplankton in the Jiaozhou Bay. *Acta Oceanol. Sin.*, **22(Suppl.)**, 293–299 (in Chinese).

Sun, J., Liu, D. Y. and Qian, S. B. (2001) Preliminary study on the seasonal succession and development pathway of phytoplankton community in the Bohai Sea. *Acta Oceanol. Sin.*, **20**, 251–260.

Taguchi, S. (1976) Relationships between photosynthesis and cell size of marine diatoms. *J. Phycol.*, **12**, 185–189.

Tang, E. P. Y. (1995) The allometry of algal growth rates. *J. Plankton Res.*, **17**, 1325–1335.

Tomas, C. R. (ed.) (1997) *Identifying Marine Phytoplankton*. Academic Press, San Diego, CA.

Utermöhl, H. (1958) Zur Vervolkommung der quantitativen Phytoplankton-Methodik. *Mitt. Int. Ver. Theor. Angew. Limnol.*, **9**, 1–38 (in German).

Verity, P. G. and Sieracki, M. E. (1993) Use of color image analysis and epifluorescence microscopy to measure plankton biomass. In Kemp, P. F., Sherr, B. F., Sherr, E. B. and Cole, J. J. (eds), *Handbook of Methods in Aquatic Microbial Ecology*. Lewis Publishers, Boca Raton, FL, pp. 327–338.

Verity, P. G., Robertson, C. Y., Tronzo, C. R., Andrews, M. G., Nelson, J. R. and Sieracki, M. E. (1992) Relationships between cell volume and the carbon and nitrogen content of marine photosynthetic nanoplankton. *Limnol. Oceanogr.*, **37**, 1434–1446.

Vilicic, D. (1985) An examination of cell volume in dominant phytoplankton species of the central and southern Adriatic Sea. *Int. Rev. Ges. Hydrobiol.*, **70**, 829–843.

Wheeler, P. A. (1999) Cell geometry revisited: realistic shapes and accurate determination of cell volume and surface area from microscopic measurements. *J. Phycol.*, **35**, 209–210.

Willén, E. (1976) A simplified method of phytoplankton counting. *Br. Phycol. J.*, **11**, 265–278.

Wood, A. M., Horan, P. K., Muirhead, K., Phinney, D. A., Yentsch, C. M. and Waterbury, J. B. (1985) Discrimination between pigment types of marine *Synechococcus* spp. by scanning spectroscopy, epifluorescence microscopy, and flow cytometry. *Limnol. Oceanogr.*, **30**, 1303–1315.

Yamaji, I. (1991) *Illustrations of the Marine Plankton of Japan*. Hoikusha Publishing Co., Osaka.

Young, J. R. and Ziveri, P. (2000) Calculation of coccolith volume and its use in calibration of carbonate flux estimates. *Deep-Sea Res.*, **47**, 1679–1700.